

THE PENNSYLVANIA STATE UNIVERSITY  
SCHREYER HONORS COLLEGE

DEPARTMENT OF ASTRONOMY & ASTROPHYSICS

THE EXOPLANET ORBIT DATABASE

EUNKYU HAN  
Fall 2012

A thesis  
submitted in partial fulfillment  
of the requirements  
for baccalaureate degrees  
in Astronomy & Astrophysics and Physics with honors in Astronomy & Astrophysics

Reviewed and approved\* by the following:

Jason T. Wright  
Associate Professor of Astronomy and Astrophysics  
Thesis Supervisor

William N. Brandt  
Distinguished Professor of Astronomy and Astrophysics

\* Signatures are on file in the Schreyer Honors College.

# Abstract

I report a series of updates and enhancements on the Exoplanet Orbit Database (EOD), which contains peer-reviewed orbital and transit parameters of exoplanets and stellar parameters of their host stars. Since December 2010, the EOD expanded from 427 planets to 640 planets, as of September 2012. The EOD can be explored through the Exoplanet Data Explorer Plotter and Table, available at <http://exoplanets.org>. I have used a program called boottran which uses radial velocity data to calculate transit times and secondary eclipse times with robust bootstrapped uncertainties, which I have made publicly available at [exoplanets.org](http://exoplanets.org). boottran calculates robust predicted transit dates with uncertainties for the next 10 years for long period planets not known to transit. I used data taken from published peer-reviewed papers and new data from the California Planet Survey for our ephemerides and for radial velocity plots on [exoplanets.org](http://exoplanets.org). Transit Ephemeris Refinement and Monitoring Survey (TERMS) uses these ephemerides to plan photometric observations of the stars. To improve the EOD, I have added fields for surface gravity, transit duration ( $T_{14}$ ), impact parameter ( $b$ ) and their uncertainties. I also have added transit parameters including secondary eclipse depth at multiple bands and Rossiter-McLaughlin spin-orbit misalignment measurements.

# Table of Contents

List of Figures	iv
List of Tables	v
Chapter 1	
The Exoplanet Orbit Database and .pln files	1
1.1 What is the EOD?	1
1.2 What is a .pln file?	1
1.3 Asymmetric uncertainties	1
Chapter 2	
Impact parameter ( $b$ ), orbital inclination ( $i$ ), and orbit-to-stellar radius ratio ( $a/R_*$ )	3
Chapter 3	
boottran	5
3.1 What is boottran?	5
3.2 How does boottran work?	5
Chapter 4	
$\log g$	6
4.1 What is $\log g$ ?	6
4.2 How is $\log g$ calculated?	6
Chapter 5	
RV plots	8
5.1 What is the radial velocity method?	8
5.2 How is the radial velocity calculated?	8
Chapter 6	
Transit	10
6.1 Transit ephemerides	10
6.1.1 Transit Ephemeris Refinement and Monitoring Survey	10
6.1.2 What is a transit ephemeris?	10
6.2 $T_{14}$ , transit duration	10
6.2.1 What is $T_{14}$ ?	10
6.3 Primary Transit	11

6.3.1	What is a primary transit? . . . . .	11
6.3.2	What do astronomers observe? . . . . .	11
6.4	Secondary Eclipse . . . . .	12
6.4.1	What is a secondary eclipse? . . . . .	12
6.4.2	What do astronomers observe? . . . . .	12
6.5	Rossiter-McLaughlin effect . . . . .	14
6.5.1	What is the Rossiter-McLaughlin effect? . . . . .	14
6.5.2	Why is the Rossiter-McLaughlin effect important? . . . . .	15
<b>Chapter 7</b>		
	<b>How the EOD and exoplanets.org were implemented by the author</b>	<b>17</b>
7.1	Asymmetric uncertainty update . . . . .	17
7.2	self-consistency among $b$ , $a/R_*$ , and $i$ . . . . .	17
7.3	Surface gravity update . . . . .	18
7.4	Radial velocity plot . . . . .	18
7.5	Transit ephemerides calculation . . . . .	18
7.6	$T_{14}$ calculation . . . . .	19
7.7	Incorporation of the Rossiter-McLaughlin effect into the EOD . . . . .	20
<b>Bibliography</b>		<b>23</b>

# List of Figures

1.1	Sample pln file in an emacs text editor window. Note asymmetric uncertainty fields for ECC . . . . .	2
2.1	Schematic diagram showing the relationships among $b$ , $a r_*$ , and $\cos i$ . The orange circle represents the planet and the blue circle represents the star. . . . .	4
6.1	Schematic diagram of transit light curve and its corresponding geometry of the planet and the star. First to forth contacts are labeled. . . . .	11
6.2	Schematic diagram of orbital motion of an exoplanet system . . . . .	12
6.3	Schematic diagram of light curve of primary transit and secondary eclipse . . . .	14
6.4	Schematic diagram of primary transit and Rossiter-McLaughlin effect . . . . .	15
6.5	Line shape vs time graph. Black line indicates the center of the disk, red line indicates red shifted limb of the star, and blue line indicates blue shifted limb of the star. This results in a velocity anomaly. . . . .	16
7.1	Sample radial velocity file . . . . .	19
7.2	Sample transit ephemeris data file . . . . .	20
7.3	Calculated $T_{14}$ and the relative error to the data from peer reviewed paper. Outliers were inspected for possible data errors. . . . .	21
7.4	Rossiter-McLaughlin effect on TrES-1 b . . . . .	22

# List of Tables

7.1	Table containing the top five exoplanetary system with the strongest dominant Rossiter-McLaughlin effect . . . . .	22
-----	--	----

# The Exoplanet Orbit Database and .pln files

## 1.1 What is the EOD?

The Exoplanet Orbit Database collects orbital and stellar parameters of all known exoplanets orbiting normal stars with good orbits reported in the peer-reviewed literature. Each planet in the EOD is stored as a text file containing the orbital parameters of the planet, orbital fit parameters, transit parameters, and stellar properties. Wright et al (2011) explains details about the EOD [1].

The EOD can be navigated through the Exoplanet Data Explorer (EDE) Plotter and Table, available at <http://exoplanets.org>. Astronomers worldwide regularly use the EOD; [exoplanets.org](http://exoplanets.org) receives roughly 1000 unique visitors each week.

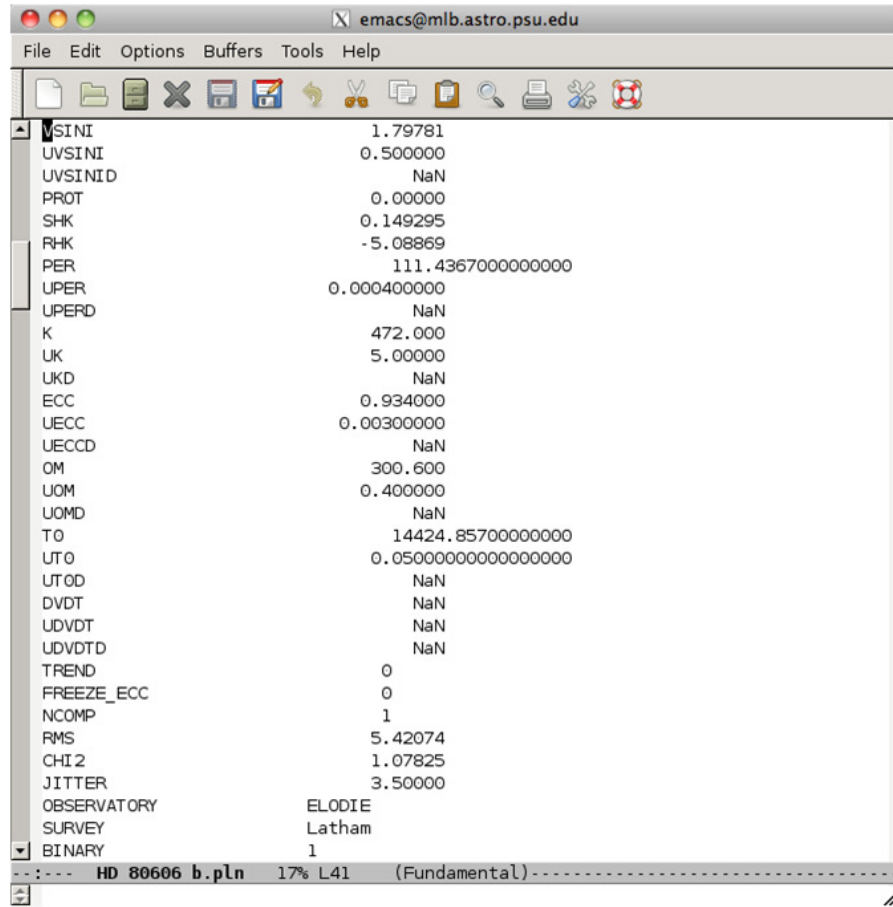
## 1.2 What is a .pln file?

Each planet in the Exoplanet Orbit Database (EOD) is stored as a flat text file that contains the orbital parameters of the planet, orbital fit parameters, stellar parameters as well as stellar properties. The files are stored with .pln extension. All parameters are from the peer-reviewed literature.

IDL, the Interactive Data Language, is a programming language that astronomers use for data analysis.

## 1.3 Asymmetric uncertainties

The EOD stores uncertainties as UX. For asymmetric uncertainties, the upper limit is given by UXD, and the lower by UXD-2\*UX where X is a parameter name. If uncertainty is



VSINI	1.79781
UVSINI	0.500000
UVSINID	NaN
PROT	0.00000
SHK	0.149295
RHK	-5.08869
PER	111.43670000000000
UPER	0.000400000
UPERD	NaN
K	472.000
UK	5.00000
UKD	NaN
ECC	0.934000
UECC	0.00300000
UECCD	NaN
OM	300.600
UOM	0.400000
UOMD	NaN
TO	14424.857000000000
UTO	0.05000000000000000
UTOD	NaN
DVDT	NaN
UDVDT	NaN
UDVDTD	NaN
TREND	0
FREEZE_ECC	0
NCOMP	1
RMS	5.42074
CHI2	1.07825
JITTER	3.50000
OBSERVATORY	ELODIE
SURVEY	Latham
BINARY	1

HD 80606 b.pln 17% L41 (Fundamental)

**Figure 1.1.** Sample pln file in an emacs text editor window. Note asymmetric uncertainty fields for ECC

symmetric, UXD = NaN. For example, in Figure 1.1, the asymmetric error in ECC is given by UECCD.



## Impact parameter ( $b$ ), orbital inclination ( $i$ ), and orbit-to-stellar radius ratio ( $a/R_*$ )

The impact parameter is the projected distance between the center of the stellar disc and the center of the planet disc at conjunction. The orbital inclination ( $i$ ) is the angle of the orbital plane of the planet relative to the plane perpendicular to the line-of-sight to the star. An inclination of  $0^\circ$  is a face-on counter-clockwise orbit, and  $90^\circ$  is an edge-on orbit. The orbit-to-stellar radius ratio,  $a/R_*$ , AR in the EOD is the ratio between the planet's orbital semi-major axis and the stellar radius. Impact parameter ( $b$ ) and orbital inclination ( $i$ ) determines transit light curve shapes. For a circular orbit, which most transiting planets have, the impact parameter  $b$  is related to the other parameters as  $b = a/R_* \cos i$ .

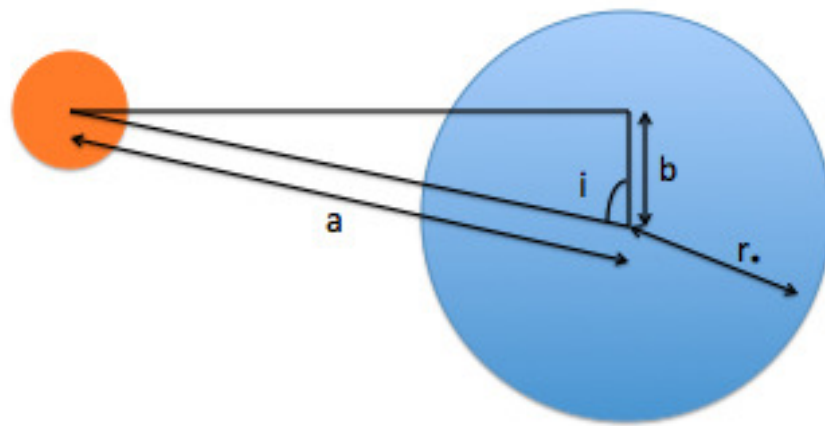


**Figure 2.1.** Schematic diagram showing the relationships among  $b$ ,  $a$ ,  $r_*$ , and  $\cos i$ . The orange circle represents the planet and the blue circle represents the star.

# Chapter 3

## boottran

### 3.1 What is boottran?

`boottran`<sup>1</sup> is a program written by Sharon (Xuesong) Wang in 2012 [2] that calculates the transit time for a planet and its uncertainties from its radial velocities. This program calls the `rvlin` package, which fits an arbitrary number of Keplerian curves to RV data. The `rvlin` package can take data from multiple telescopes. `boottran` returns uncertainties for all of `rvlin`'s orbital parameters with the time of transit. It is a published procedure and details can be found in Wright & Howard 2009 [3].

### 3.2 How does boottran work?

When `rvlin`<sup>1</sup> returns a fitted set of orbital parameters, `boottran` uses a bootstrapping algorithm to determine the uncertainties in the parameters; it takes the orbital solution, subtracts the planet off, resamples the residuals, and creates an artificial data set. `boottran` repeats the bootstrapping algorithm 1,000 times and produces different data sets. The created data sets look very similar to the original radial velocities. Then it uses the ensemble of data sets and looks at the spread of the obtained parameters, which are the uncertainties. `boottran` is robust to outliers because it disregards any outlier.

`boottran` returns orbital parameters with an extra parameter, the transit time, which we use to predict the transit date of exoplanets known to transit. If no date is entered, `boottran` calculates the next transit times from today.

---

<sup>1</sup>Available at <http://exoplanets.org/code>

# Chapter 4

## $\log g$

### 4.1 What is $\log g$ ?

The surface gravity,  $g$ , of a star is the gravitational acceleration experienced at the surface of the star. It is a function of mass and radius. In the EOD, we record  $\log g$ , the logarithm of the gravity of parent star in c.g.s units.

### 4.2 How is $\log g$ calculated?

The surface gravity of a star can be calculated from Newton's 2<sup>nd</sup> Law of Motion and Law of Universal Gravitation.

$$F = \frac{GMm}{r^2}$$

$$F = mg \tag{4.1}$$

$$\tag{4.2}$$

Equating them gives

$$g_{\text{surf}*} = \frac{GM_*}{R_*^2} \tag{4.3}$$

The subscript \* indicates the star. The mass and radius of a star are in the c.g.s for this calculation. Thus, it is possible to calculate the surface gravity of a star in the units of solar surface gravity in those cases where a spectroscopic  $\log g$  is not given. Taking the log of  $g$  gives,

$$\log g_* = \log \left( \frac{GM_*}{R_*^2} \right) \tag{4.4}$$

where  $M_*$  and  $R_*$  are in c.g.s. Furthermore, by propagating errors, the uncertainty in the surface gravity can be calculated.

$$\begin{aligned}
\log g &= \log \frac{\text{GM}_*^2}{R_*} \\
&= \log \left( \frac{(M_*/M_\odot)}{(R_*/R_\odot)^2} \frac{\text{GM}_\odot}{R_\odot^2} \right) \\
&= \log \left( \frac{(M_*/M_\odot)}{(R_*/R_\odot)^2} \right) + \log g_\odot
\end{aligned} \tag{4.5}$$

$$\begin{aligned}
\sigma_{\log g}^2 &= \left( \frac{\partial \log g}{\partial g} \right)^2 \sigma_{g^2} \\
&= \left( \frac{1}{\ln 10} \right)^2 \left( \frac{\partial \ln g}{\partial g} \right)^2 \left[ \left( \frac{\partial g}{\partial M_*} \right)^2 \sigma_{M_*}^2 + \left( \frac{\partial g}{\partial R_*} \right)^2 \sigma_{R_*}^2 \right] \\
&= (\ln 10)^{-2} \left[ \left( \frac{G}{R_*^2} \right)^2 \sigma_{M_*}^2 + \left( -\frac{2\text{GM}_*}{R_*^3} \right)^2 \sigma_{R_*}^2 \right] \left( \frac{\text{GM}_*}{R_*^2} \right)^{-2} \\
&= (\ln 10)^{-2} \left[ \left( \frac{\sigma_{M_*}}{M_*} \right)^2 + 4 \left( \frac{\sigma_{R_*}}{R_*} \right)^2 \right]
\end{aligned} \tag{4.6}$$

In the above equation,  $\log g_\odot$  is 4.43. This means that if the mass of a star is 10 times the solar mass and the radius is 10 times the solar radius,  $\log g$  of the star is 3.43.

## RV plots

### 5.1 What is the radial velocity method?

The radial velocity of an exoplanet enables astronomers to obtain information about the orbital shape, period, distance and mass [4]. The radial motion of a star can be measured using Doppler shift. 6 orbital parameters are observed through this method:  $P$ ,  $K$ ,  $T_0$ ,  $e$ ,  $\omega$ , and  $\gamma$ .  $P$  is period of the orbital motion in days,  $K$  is the semi-amplitude of stellar reflex motion in m/s, and  $T_0$  is epoch of periastron passage which we measure in units of HJD-2440000. They set the period, phase, and amplitude of an RV curve.  $e$ , the orbital eccentricity, and  $\omega$ , the argument of periastron, set the shape of the curve.  $\gamma$  is the velocity of the center of mass of the star-planet system. In the EOD, we record  $\omega$  in units of degrees.

### 5.2 How is the radial velocity calculated?

These 6 orbital parameters determine the radial velocity curve. From Newton's Law of motion and assuming a circular orbit,

$$F = \frac{GM_*m_p}{r_p^2} \quad (5.1)$$

and we set  $r_p = a$ .

$$F = \frac{M_*V_*^2}{R_*} \quad (5.2)$$

Equating them gives

$$\frac{Gm_p}{r_p^2} = \frac{V_*^2}{R_*} \quad (5.3)$$

Moreover, from the center of mass equation,

$$R_* = \frac{m_p r_p}{M_*} \quad (5.4)$$

Putting eq(5.4) into (5.3) gives the stellar velocity.

$$V_*^2 = \frac{Gm_p^2}{M_*r_p} \quad (5.5)$$

As shown in the equation, the stellar velocity increases as the mass of the planet increases and decreases as the square root of stellar mass and the square root of the distance of the planet increase.

# Chapter 6

## Transit

### 6.1 Transit ephemerides

#### 6.1.1 Transit Ephemeris Refinement and Monitoring Survey

The Transit Ephemeris Refinement and Monitoring Survey (TERMS, PI: Stephen Kane), is a project that aims to detect transiting planets [5]. TERMS also detects planets not yet known to transit. We re-determined the orbital parameters of the known exoplanets with additional data provided by Keck and Lick observatories. With the ephemeris, astronomers monitor the planet during the predicted transit dates.

#### 6.1.2 What is a transit ephemeris?

Transit ephemerides are the tables of times and positions of exoplanetary systems. It is important to have precise transit ephemerides because this information is the most essential factor for a successful observation of the transit of a known exoplanet.

### 6.2 $T_{14}$ , transit duration

#### 6.2.1 What is $T_{14}$ ?

$T_{14}$  is time of transit from the first contact to the fourth contact. In the EOD, its unit is in days, and it is one of the transit parameters. Figure 6.1 shows transit light curve and the corresponding geometry of the planet and the star.



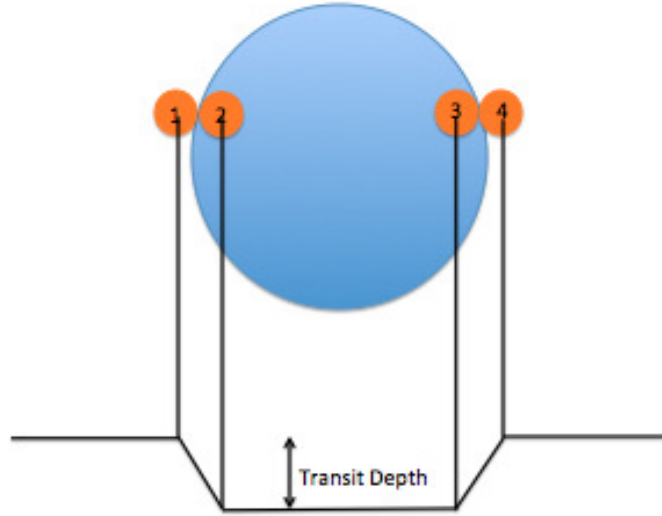


**Figure 6.1.** Schematic diagram of transit light curve and its corresponding geometry of the planet and the star. First to forth contacts are labeled.

## 6.3 Primary Transit

### 6.3.1 What is a primary transit?

Primary Transit of a planet refers to a passage of the planet in front of the parent star (i.e.  $i = 90^\circ$ ). This can be observed only when the planet's orbital plane aligns with the line of sight. The event can be recorded photometrically as done by Charbonneau et al (2005) [6]. When a planet transits in front of the parent star, it blocks starlight, and the amount blocked is determined to first order by the planet to star area ratio.

### 6.3.2 What do astronomers observe?

During the transit, astronomers measure the flux of the star and plot the relative flux versus time. Because of the decreased amount of flux recorded starting from ingress (entering point) to egress (ending point), there is a noticeable dip in the plot. The time that the planet takes to go from ingress to egress is called  $T_{14}$ , and the dip is “depth”, which can be roughly calculated from  $(\frac{R_p}{R_*})^2$ . Given the size of the star, transits of exoplanets provide information about the radius of the exoplanet. Astronomers can also calculate the impact parameter  $b$  from  $b = a/R_* \cos i$  for circular orbits ( $e = 0$ ). Here,  $a$  is the semi-major axis of the planet's orbit,  $R_*$  is the radius of the star, and  $i$  is the orbital inclination.

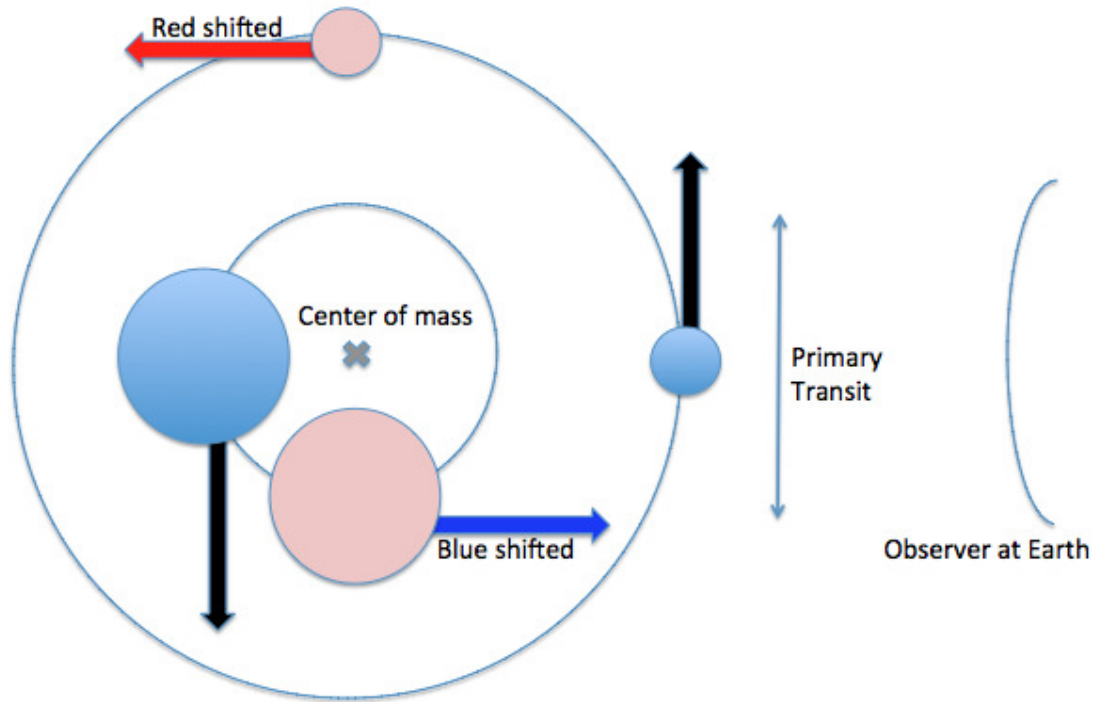


**Figure 6.2.** Schematic diagram of orbital motion of an exoplanet system

## 6.4 Secondary Eclipse

### 6.4.1 What is a secondary eclipse?

The secondary eclipse of a planet refers to a passage of a planet behind the parent star. When the planet goes behind the star, the total radiation from the system drops by the amount that the planet contributes. Moreover, the amount that gets dropped is determined by the brightness and the relative sizes of the planet and the star.

### 6.4.2 What do astronomers observe?

During the secondary eclipse, astronomers are able to obtain the flux spectrum of the star itself because there is no flux coming from the planet. Thus, astronomers are able to study the planetary atmosphere from the secondary eclipse because the flux spectrum of the planet can be obtained by dividing the spectrum of the star from the spectrum of the star with the planet, which can be obtained just before and after the eclipse. Once the planetary flux spectrum graph is extracted, the chemical composition of the planetary atmosphere and temperature gradient (if the spectrum lies in the infrared) or albedo (if the spectrum lies in the visible wavelength) can be studied.

For a circular orbit where the orbital plane aligns with the line of sight, the secondary eclipse occurs half of an orbital period after transit.

The blackbody radiation equation gives the energy per unit time emitted per unit area per unit frequency:

$$B_\nu = \frac{2h\nu^3}{c^2} \frac{1}{e^{\frac{h\nu}{kT}} - 1} \quad (6.1)$$

In the Rayleigh-Jeans limit, which is appropriate for the infrared, the stars emit the specific flux, which depends on the surface temperature as shown by eq (6.3).

$$\begin{aligned} B_\nu(\nu \rightarrow 0) &= \frac{2h\nu^3}{c^2} \frac{kT}{h\nu} \\ &= \frac{2\nu^2}{c^2} kT \end{aligned} \quad (6.2)$$

Moreover, the total luminosity radiated by an object ( $L$ ) and the flux recorded by an observer at distance  $d$  and  $F$  can also be calculated from Stefan Boltzmann's equation:

$$\begin{aligned} L &= 4\sigma T^4 \pi R^2 \\ F &= \frac{4\sigma T^4 \pi R^2}{4\pi d^2} \\ &= \frac{L}{\pi d^2} \end{aligned} \quad (6.3)$$

With these two equations, astronomers can use transit light curve to study how flux decreases when the secondary eclipse occurs. As discussed above, the depth of transit is calculated roughly from  $(\frac{R_p}{R_*})^2$ . Moreover, to determine the light curve shapes for the secondary eclipse, astronomers consider how much radiation was contributed by the planet and calculate the difference in radiation and flux. Given the surface temperatures of the star and the planet, we can approximate the ratio of planet to star flux. From eq (6.4)

$$\frac{F_p}{F_*} = \left(\frac{R_p}{R_*}\right)^2 \left(\frac{T_p}{T_*}\right) \quad (6.4)$$

For example, let us assume that the planet has a radius of  $0.1R_\odot$  and a surface temperature of  $T = 1,000K$ , while the star has a radius of  $1R_\odot$  and a surface temperature of  $T = 5,000K$ . Then, during the eclipse, the system gets dimmer by:

$$\begin{aligned} \text{Transit} : \left(\frac{R_p}{R_*}\right)^2 &= \left(\frac{0.1R_\odot}{1R_\odot}\right)^2 = 1\% \\ \text{Secondary} : \left(\frac{R_p}{R_*}\right)^2 \left(\frac{T_p}{T_*}\right) &= 1\% \times \frac{1000K}{5000K} = 0.2\% \end{aligned} \quad (6.5)$$

Figure 6.3 shows a schematic diagram of light curve or primary transit and secondary eclipse.

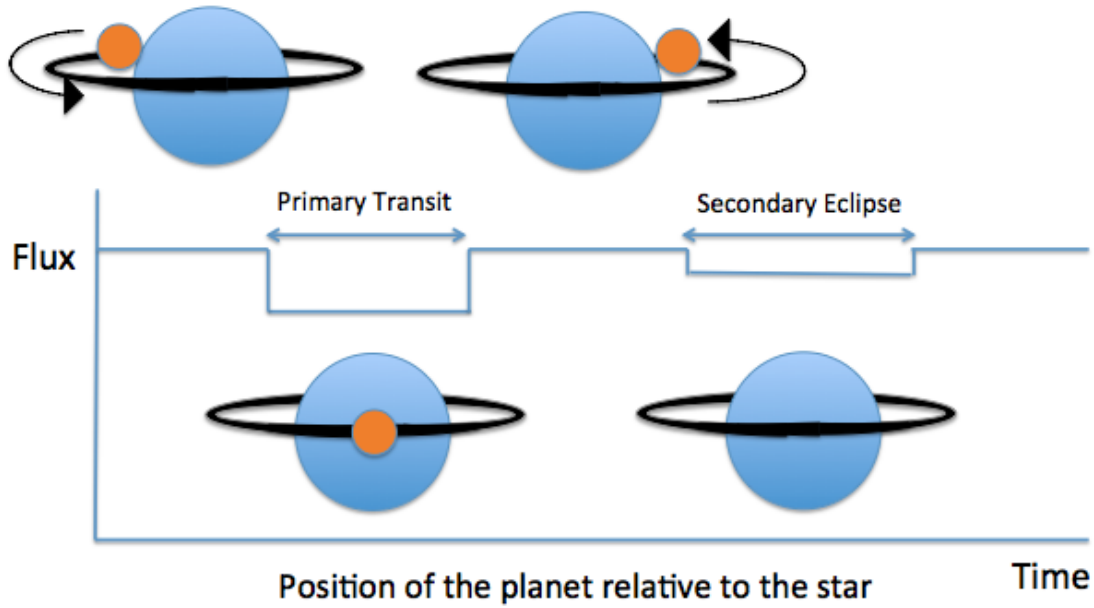


**Figure 6.3.** Schematic diagram of light curve of primary transit and secondary eclipse

Secondary eclipse depth is usually measured in the infrared, especially in the J, H, and K bands. Sometimes it is also measured in the Y band, but astronomers do not care much about the Y band compared to the other three bands because not enough photons are observed in the Y band due to the absorption from atmosphere. To measure transits, astronomers need to have a precision of 1/100, whereas for the secondary eclipse (or transmission spectrum), precision of 1/10,000 is required. This means it is much harder to detect the secondary eclipse depths or transmission spectra compared to just transit.

## 6.5 Rossiter-McLaughlin effect

### 6.5.1 What is the Rossiter-McLaughlin effect?

During transit, the planet blocks the light coming from different regions of the star, and due to Doppler shift, the RV looks distorted. This phenomenon was originally reported by two independent papers by R.A. Rossiter and D.B. McLaughlin, who observed the distortion effect in eclipsing binary systems in 1924 [7],[8]. For exoplanet systems, the Rossiter-McLaughlin effect is observed when a planet transits. The Rossiter-McLaughlin effect together with proper Keplerian fit allows astronomers to obtain the projected angle between the planetary orbital axis and the stellar spin axis.

### 6.5.2 Why is the Rossiter-McLaughlin effect important?

The importance of studying the Rossiter-McLaughlin effect comes from the fact that it provides the angle  $\lambda$  between the stellar rotation axis. The expected distribution of  $\lambda$  values differs according to how and where hot jupiters are formed and how they migrate. Thus, studying the ensemble of values of  $\lambda$  provides astronomers clues to distinguish between different planet formation and migration processes. The ensemble of  $\lambda$  values that we measure across all of the planets tells us how the planets migrated. Ohta et al (2005) [9] derived an analytic formula that calculates the velocity anomalies due to the Rossiter-McLaughlin effect.

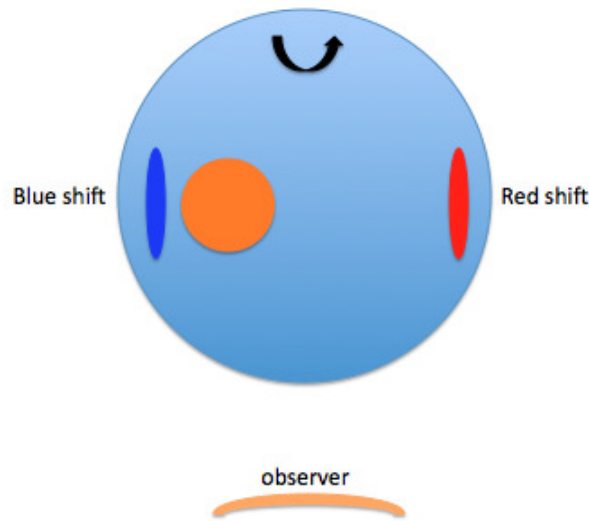


**Figure 6.4.** Schematic diagram of primary transit and Rossiter-McLaughlin effect

As shown in Figure 6.4, if the star rotates, the left side is blue-shifted while the right side is red-shifted. This is also reflected in the line shape versus time graph.

As shown in Figure 6.5, when the star rotates, the observer measures red or blue shifted  $F(\lambda)$  from different limbs of the star. Taking the stellar rotation into account, when the planet transits in front of the star, it blocks light from the star. When a planet orbiting prograde just enters the transit, it blocks light from the left part, and the blue shifted flux is not measured by the observer. In this case, the blue lines in Figure 6.5 will be removed, leaving only black and red lines. When the planet is about to leave the transit phase, it blocks light from the right part, and the red shifted flux is not measured, leaving only blue and black lines. This is interpreted by Doppler codes as an anomalous Doppler effect, as shown in Figure 7.4.

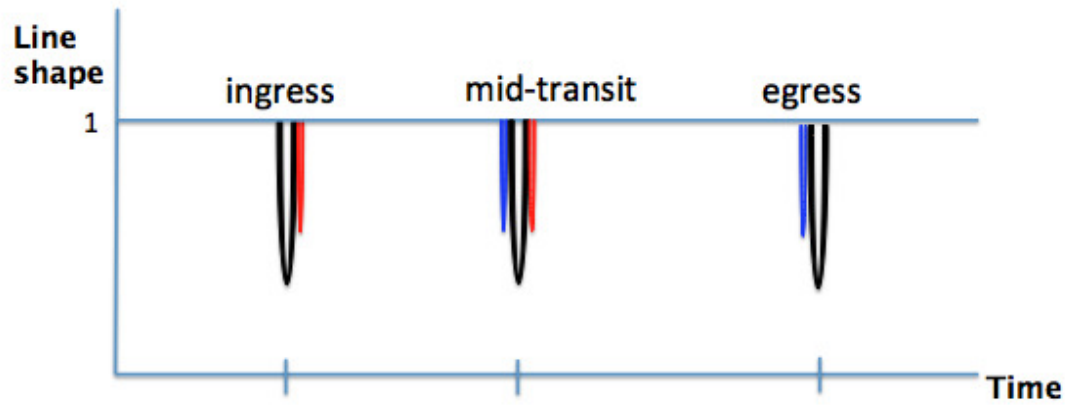


**Figure 6.5.** Line shape vs time graph. Black line indicates the center of the disk, red line indicates red shifted limb of the star, and blue line indicates blue shifted limb of the star. This results in a velocity anomaly.

## How the EOD and exoplanets.org were implemented by the author

Since 2009, I have expanded the EOD from over 400 planets to more than 600. For the newly discovered exoplanets, I have put in orbital parameters of the planet, orbital fit parameters, stellar parameters, and stellar properties from the peer-reviewed literature. I have edited .pln files whenever changes are required by a new orbital fit in the literature. To commit the changes and convert the files to a readable format for exoplanets.org, I have written IDL programs.

### 7.1 Asymmetric uncertainty update

For asymmetric uncertainties, I have searched the EOD where  $X - UX < 0$ . For this case, I have set the upper limit by UXD, which was given by the peer-reviewed paper and the lower by  $UXD - 2*UX$  where X is a parameter name.

### 7.2 self-consistency among $b$ , $a/R_*$ , and $i$

I have searched the EOD for planets with parameters inconsistent with  $b = a/R_* \cos i$  for the circular orbit case by plotting  $b$  versus  $a/R_* \cos i$ . All the outliers to the straight line were selected, and each system was reviewed to find the cause of the difference. For some systems, it was simply because they were not following the  $b = a/R_* \cos i$  definition. The parameters were estimated inconsistently and the orbit was not circular. There were some cases where one parameter among  $b$ ,  $a/R_*$ , and  $i$  was undefined, since it was not given by the referenced paper. In other cases, there was an error in the EOD. This procedure allowed me to correct these errors. After correcting these problems, I used EDE to find the planets whose lower limits for  $b$  were less

than 0. I repaired these errors in the EOD by calculating appropriate value for  $0 = \text{UBD} - 2 * \text{UB} + \text{B}$  where UBD is the asymmetric error, UB is the uncertainty in impact parameter, and B is impact parameter. Other than this case, UBD was set to  $\text{B} - \text{UB}$ .

### 7.3 Surface gravity update

In the EOD, there were cases where the peer-reviewed literature provided the stellar mass and radius but not the surface gravity. I have searched the EOD where MSTAR and RSTAR are finite, but LOGG is not given. By using eq (7.1) and (7.2), I have calculated LOGG and ULOGG, which are both in solar units.

$$\text{LOGG} = \log \frac{G * \text{MSTAR}^2}{\text{RSTAR}} + 4.43 \quad (7.1)$$

$$\text{ULOGG} = \frac{\sqrt{\left(\frac{\text{UMSTAR}}{\text{MSTAR}}\right)^2 + 4 \left(\frac{\text{URSTAR}}{\text{RSTAR}}\right)^2}}{\ln 10} \quad (7.2)$$

### 7.4 Radial velocity plot

One of the features of the EOD is that we have a radial velocity plot for every star. I made over 100 radial velocity plots. I produced radial velocity plots using **cneplot**, which plots RV curves from an RV data set. I obtained these RVs from either the Exoplanet Archive at NExSCI, or from RVs measured by the California Planet Survey at HET, Keck, and Lick Observatories. As **cneplot** reads off the data set, it reads the corresponding planet's pln file in our database. Based on the orbital parameters stored in the pln file, **cneplot** plots up the RV curve. If a dataset file is missing from the Archive, I referred back to the paper and downloaded the RVs, stored them in a plain text file, and read the file using the **readcol** function in IDL ASTROLIB<sup>1</sup>. I entered more than 100 radial velocities plots, and the database is now approximately 50% complete. A sample radial velocity plot that I made is shown in Figure 7.1.

### 7.5 Transit ephemerides calculation

In order to calculate transit ephemerides, I wrote a program called **orgdat**, which uses **boottran** to calculate the predicted transit dates based on the orbital parameters available from the EOD. **orgdat** organizes data of the transiting planets as well as the next transiting dates with their uncertainties after the day it is calculated. Furthermore, it also calculates the next five secondary eclipse (see section 6.4) dates and saves all the data in a plain text file. The

---

<sup>1</sup><http://idlastro.gsfc.nasa.gov/>



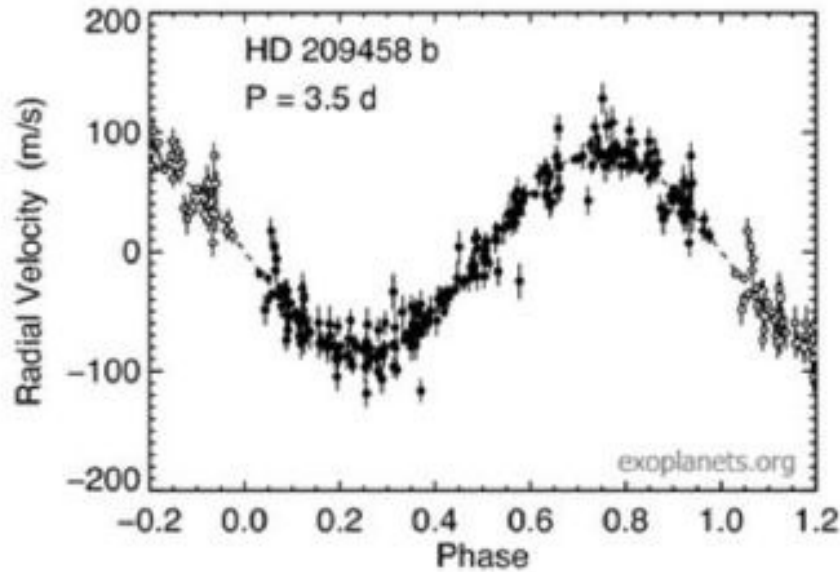


**Figure 7.1.** Sample radial velocity file

transiting dates and their uncertainties are calculated in Julian dates and are then converted into human-readable dates.

For TERMS, I wrote another program called `transepm`, which is similar to `orgdat` but produces a file for each system. `transepm` takes input planets, and when specified to call `boottran`, it runs `boottran` to calculate predicted transit dates and the secondary eclipse dates with uncertainties for the next 10 years. Thus, the number of transit dates calculated depends on the period of the planet; with a longer period, the planet will not transit frequently.

Once the calculation is done, `transepm` produces a data file to store the ephemeris. The file contains the name of the planet, its orbital parameters ( $P, e, K, \omega, T_0$ ), and the date the file was produced. The date is important because `boottran` calculates the next transiting dates from the day it is calculated. `transepm` also provides predicted transit dates with uncertainties and predicted secondary eclipse dates with uncertainties. A sample data file for TERMS is shown in Figure 7.2.

## 7.6 $T_{14}$ calculation

I wrote a program called `calct14`, which calculates  $T_{14}$  and its uncertainty,  $\sigma T_{14}$ . The relevant equation is taken from Seager et al (2003)[10]. Period, inclination angle, depth, and the ratio between the semi-major axis and the star radius, go into the equation. This data comes from .pln files, which are text files that contain orbital and stellar parameters from the peer-reviewed literature.

Figure 7.2 shows a screenshot of an Emacs window displaying a sample transit ephemeris data file. The window title is 'emacs@mb.astro.psu.edu'. The file is 'HD 156846.tranepm.dat'. The data includes orbital parameters like P, UPER, Tp, Utp, Ue, Uq, Uqdeg, UqM, K, UK, gamma, Ugama, dv/dt, Udv/dt, and seTp. It also lists transit dates in JD and Gregorian calendar, along with uncertainties and secondary eclipse dates.

Figure 7.2. Sample transit ephemeris data file

Then I calculated all transiting planets'  $T_{14}$  values and plotted  $T_{14_{\text{calculated}}}$  versus  $T_{14_{\text{paper}}}$ , as well as the relative error to look for discrepancies.

The equation for the transit duration is provided below:

$$t_T = \frac{P}{\pi} \arcsin \sqrt{\frac{R_* (1 + R_p/R_*)^2 - (a/R_* \cos i)^2}{1 - \cos^2 i}} \quad (7.3)$$

Then the relative error can be calculated from

$$T_{14_{\text{relative}}} = \frac{t_T - T_{14_{\text{paper}}}}{T_{14_{\text{paper}}}} \quad (7.4)$$

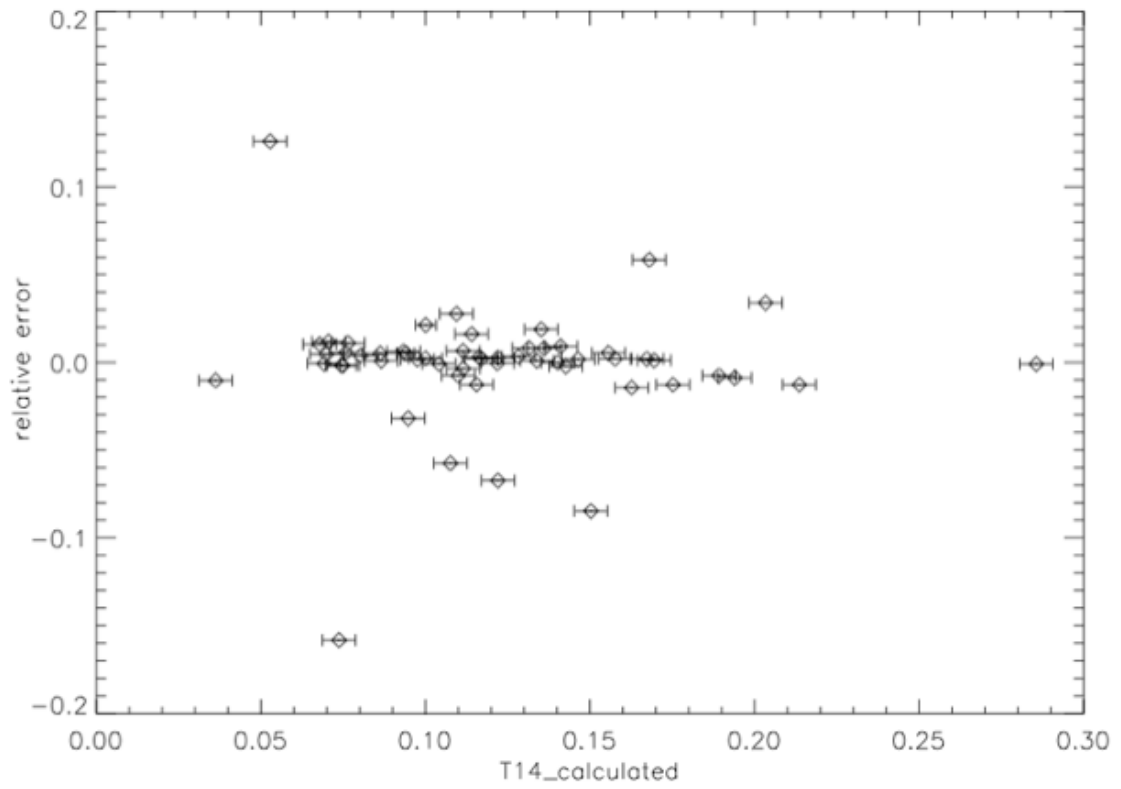
There were six systems with relative error within 0.05 and thirteen systems with relative error within 0.10. Other systems did not lie within the range and thus needed to be explored further to figure out what gave such a large relative error.

Figure 7.3 was used to check whether our data ( $P$ ,  $R_*$ ,  $R_p$ ,  $a$ , and  $i$ ) in the EOD are self-consistent. If the data turn out to be inconsistent, it is because either we put in wrong numbers by mistake or the paper has wrong values. For the latter case, I double checked the data with the authors. I corrected the erroneous values.

## 7.7 Incorporation of the Rossiter-McLaughlin effect into the EOD

The Rossiter-McLaughlin effect becomes dominant when the transit depth and  $v \sin i_*$  increase. Using the EOD, I found these systems that have the strongest Rossiter-McLaughlin effect by limiting  $V$  less than 13, since the effect is only measurable for bright stars and  $b$  less than 0.5. We have WASP-33 as having the most dominant Rossiter-McLaughlin effect. Figure 7.4 illustrates the Rossiter-McLaughlin effect.

I present the top five systems with dominant Rossiter-McLaughlin effects in Table 7.1. These are the 5 strongest Rossiter-McLaughlin effect and are the easiest to measure the spin-orbit misalignment. However, we have only three of them measured. This is because KELT-1 b and



**Figure 7.3.** Calculated  $T_{14}$  and the relative error to the data from peer reviewed paper. Outliers were inspected for possible data errors.

HAT-P-41 b are discovered in this year, and they are our prime targets and should be measured.

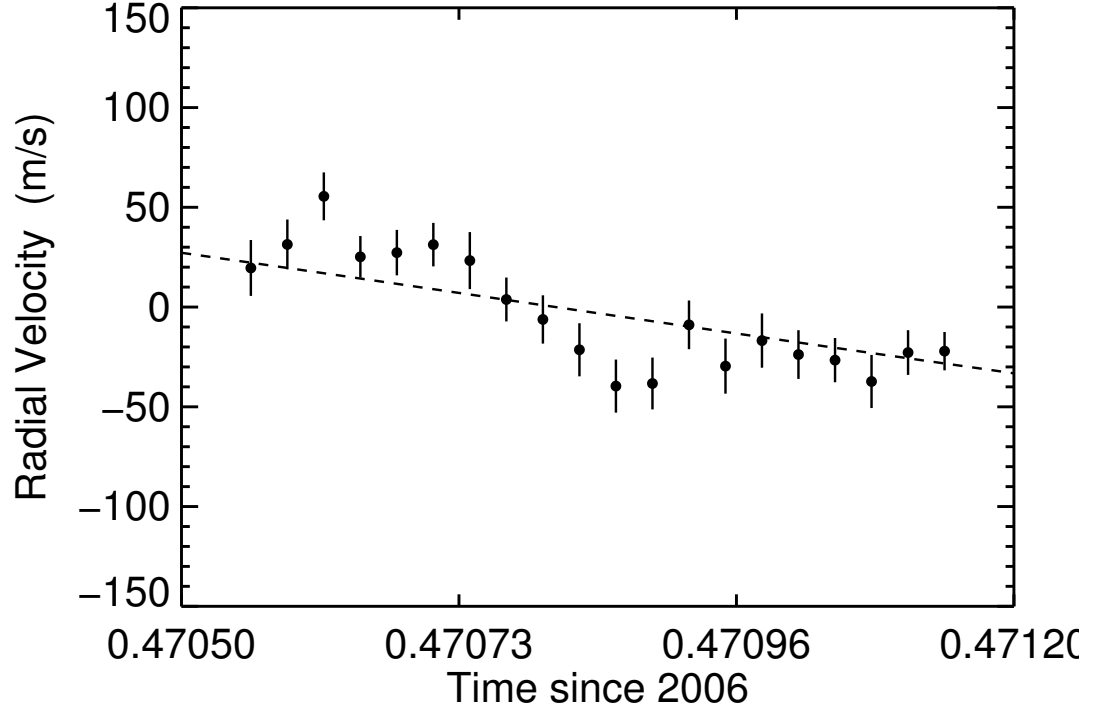


**Figure 7.4.** Rossiter-McLaughlin effect on TrES-1 b

System	Transit Depth (b)	vsini	b*vsini	Projected spin-orbit misalignment
WASP-33 b	0.01136	90.00	1.0227	-107.7
HAT-P-32 b	0.02274	21.00	0.4776	85.0
KELT-1 b	0.006086	56.00	0.3408	-
CoRoT-2 b	0.02750	11.85	0.3259	77.0
HAT-P-41 b	0.01057	19.60	0.2071	-

**Table 7.1.** Table containing the top five exoplanetary system with the strongest dominant Rossiter-McLaughlin effect

# Bibliography

- [1] WRIGHT, J. T., O. FAKHOURI, G. W. MARCY, E. HAN, Y. FENG, J. A. JOHNSON, A. W. HOWARD, D. A. FISCHER, J. A. VALENTI, J. ANDERSON, and N. PISKUNOV (2011) “The Exoplanet Orbit Database,” *Publications of the Astronomical Society of the Pacific*, **123**, pp. 412–422.
- [2] XUESONG WANG, S., J. T. WRIGHT, W. COCHRAN, S. R. KANE, G. W. HENRY, M. J. PAYNE, M. ENDL, P. J. MACQUEEN, J. A. VALENTI, V. ANTOCI, D. DRAGOMIR, J. M. MATTHEWS, A. W. HOWARD, G. W. MARCY, H. ISAACSON, E. B. FORD, S. MAHADEVAN, and K. VON BRAUN (2012) “The Discovery of HD 37605c and a Dispositive Null Detection of Transits of HD 37605b,” *Astrophysical Journal*, **761**, pp. 46–58.
- [3] WRIGHT, J. T. and A. W. HOWARD (2009) “Efficient Fitting of Multiplanet Keplerian Models to Radial Velocity and Astrometry Data,” *Astrophysical Journal*, **182**, pp. 205–215.
- [4] WRIGHT, J. T. and B. S. GAUDI (2012) “Exoplanet Detection Methods,” *ArXiv e-prints*, 1210.2471.
- [5] KANE, S. R., S. MAHADEVAN, K. VON BRAUN, G. LAUGHLIN, and D. R. CIARDI (2009) “Refining Exoplanet Ephemerides and Transit Observing Strategies,” *Publications of the Astronomical Society of the Pacific*, **121**, pp. 1386–1394.
- [6] CHARBONNEAU, D., T. M. BROWN, A. BURROWS, and G. LAUGHLIN (2007) “When Extrasolar Planets Transit Their Parent Stars,” *Protostars and Planets V*, pp. 701–716, [arXiv:astro-ph/0603376](#).
- [7] ROSSITER, R. A. (1924) “On the detection of an effect of rotation during eclipse in the velocity of the brighter component of beta Lyrae, and on the constancy of velocity of this system.” *Astrophysical Journal*, **60**, pp. 15–21.
- [8] McLAUGHLIN, D. B. (1924) “Some results of a spectrographic study of the Algol system.” *Astrophysical Journal*, **60**, pp. 22–31.
- [9] OHTA, Y., A. TARUYA, and Y. SUTO (2005) “The Rossiter-McLaughlin Effect and Analytic Radial Velocity Curves for Transiting Extrasolar Planetary Systems,” *Astrophysical Journal*, **622**, pp. 1118–1135, [arXiv:astro-ph/0410499](#).
- [10] SEAGER, S. and G. MALLÉN-ORNELAS (2003) “A Unique Solution of Planet and Star Parameters from an Extrasolar Planet Transit Light Curve,” *Astrophysical Journal*, **585**, pp. 1038–1055, [arXiv:astro-ph/0206228](#).